BREAKING THE 11 KWH/KG BARRIER

Marc Dupuis, Jonquière

It is important when performing a design study to establish a design goal. For the study presented here, the design goal was to break the 11 kWh/kg cell energy consumption barrier because it was judged to be an achievable short term design goal.

Introduction

The R&D design work presented in this article is the immediate follow-up of what was presented by the author in a paper at the 2018 TMS conference [1]. In that paper, two designs were studied. The first one is based on a cathode design where 100% of the cell current is extracted from its downstream side [2,3]. In [1], the outcome of the study is a 500 kA 100% downstream current extraction cell design operating in thermal balance at 11.2 kWh/kg. Yet in the future work section, some ideas are proposed to further reduce the cell energy consumption. Those ideas have been implemented in the present study.

In [1], the second design is based on the usage of a wider cell, idea initially presented a year ago in ALUMINIUM [4]. That wider cell is using the Reversed Compensation Current (RCC) busbar concept first shown in [5]. The outcome of the study is a 650 kA wider cell design operating in thermal balance at 11.3 kWh/kg. Again in [1] the future work section, some ideas are proposed to further reduce the cell energy consumption and those ideas have been tested in the present study as well.

Design 1: Wider 650 kA cell using RCC busbar design

In [1], it was concluded that the 2 carbon blocks per anode, 2 stubs per carbon block anode design was limiting the possibilities to further reduce the anode voltage drop. For that reason, a new anode model was developed for the current study in order to test a new 4 carbon blocks per anode, 3 stubs per carbon block anode design. Figure 1 presents the new anode model topology. The anode block surface is kept horizontal in order to simplify the model topology, a more detailed model will include extra features to minimize the carbon usage. As Table I indicates, the global anode length has remained unchanged with 4 of 1.3 m x 0.43 m carbon blocks for a total area of 2.6 m x 0.86 m per anode. Since there are 3 stubs per carbon blocks, each stub is providing current to an almost square 0.433 m x 0.43 m carbon surface area. The new stub diameter is 16 cm.

As in the initial concept presented in [4], there is a 6 cm wide channel between the front and back carbon blocks. Barry Welch who proposed to incorporate this 6 cm channel to enhance electrolyte flow and mixing now believes that 6 cm is not wide enough anymore. But in the current study, the channel width was kept the same in order to avoid having to further increase the cell which would have force an adjustment to the cathode design and to have to increase the pot to pot distance which would have force an adjustment to the busbar design. There is only a 2 cm channel between the 2 side by side carbon blocks and there is room for 36 such anodes in that wider cell.

As Figure 1 indicates, the new anode design is characterized by a very long horizontal yoke. As Figure 2 indicates, following Barry Welch's recommendation, a copper insert was inserted in that yoke. This copper insert further contributed to reduce the anode electrical resistance and hence the anode voltage drop without increasing the anode heat loss. Figure 3 is presenting the obtained temperature solution. As Table I indicated, the anode cover is 25 cm thick which is a lot but is required to reduce the anode heat loss. The anode hole design incorporates the patented idea to pass current in the horizontal contact between the stud and the carbon [6]. The anode also incorporates a non-described design feature that permits to further reduce the anode heat loss. As Table I indicates, the predicted anode voltage drop is 252 mV, a 44 mV reduction over the predicted 296 mV anode drop reported for the anode design presented in [1]. The anode panel heat loss is predicted to increase by 12 kW to 339 kW over the 327 kW predicted for the anode design presented in [1].

In [1], it was also recommended to further optimized the RCC busbar network in order to reduce even more the reported 220 mV busbar drop. As presented in Figure 5 of [1], that RCC busbar network is using a total of 6 risers, 3 on the upstream side and 3 more offset on the downstream side. Again, following Barry Welch's recommendation, that 6 risers RCC busbar network was replaced by a 8 risers RCC busbar network, 4 on the upstream side and 4 more offset on the downstream side as presented in Figure 4. As presented in Table I, the new busbar voltage drop is predicted to be reduced by 50 mV to 170 mV.

Figure 5 presents the global setup of the MHD model. Notice that MHD-Valdis doesn't support a 4 blocks per anode, 3 stubs per block anode design so a single block 8 stubs anode design was selected instead. Figures 6 to 8 present respectively the obtained BZ, bath-metal interface deformation and metal flow field. As the MHD results indicate the 8 risers RCC busbar design is even better than the 6 risers RCC busbar design. As Table I finally shows, after the change of both the anode and the busbar, the third version (right column of Table I) of the Wider cell still operating at 650 kA is predicted to operate in thermal balance dissipating only 804 kW consuming exactly 11.0 kWh/kg which is reaching but not breaking the 11.0 kWh/kg barrier!

Design 2: 520 kA cell with 100% downstream side current extraction

The reduction of the cell energy consumption is always a struggle between the reduction of the cell internal heat generation hence the reduction of the ohmic components of the cell voltage and the reduction of the cell heat loss. The struggle is coming from the fact that reducing the electrical resistance of cathode and the anode will also typically reduce the thermal resistance of those ohmic components. As a result, further reduction of the cell energy consumption can be limited by the heat production side or the heat dissipation side. For Design 1, the limitation is on the heat production side as a wider cell dissipates less heat per unit production but on the other hand its makes the reduction of the electrical resistance of the ohmic components like the busbar more challenging.

For Design 2, it is the opposite, the reduction of the ACD from 3.2 cm to 2.8 cm automatically reduces the cell internal heat generation but at 500 kA, it was not possible to find a way to operate the cell in thermal balance at a "reasonable" cell superheat. So, the cell amperage had to be increased to 520 kA in order to maintain the cell internal heat around 700 kW as indicated in Table II. Of course, this change of ACD and amperage means that the anode and cathode models must be rerun to analyze the impact of those two operational changes. These new results are also reported in Table II third column; first an increase of 10 mV for the anode drop from 238 mV to 248 mV without significant change to the anode panel heat loss. Second, on the cathode side, a small increase of 5 mV of the cathode voltage drop from 125 mV to 128 mV is obtained again without significant impact on the cathode heat loss at the expense of a slight reduction of the cell superheat from 5.4 °C to 5.3 °C. Some people would argue that it is not possible to operate a cell at such a low cell superheat, yet the author remembers having on purpose design the cell lining of the A310 cell so it would operate a 6 °C of cell liquidus superheat and the cell operated quite well at that predicted superheat and predicted ledge thickness arguably with a lot more bath volume that was the standard at the time.

The second recommendation for the "500" kA cell with 100% downstream side current extraction was the reduction of the cell center to center distance which was set at 7 meters in the previous design reported in

[1]. That number has been reduced to 6.2 meters in the current study. It was easy to significantly reduce that number because that important cell design parameter has not been previously optimized. At the same time, the busbar sections have been increased in order to further reduce the busbar drop that was already quite low due to the fact that the busbar of a cell with 100% downstream side current extraction is only constituted of anode risers. The number was kept to 6 risers, but on second tough, again it might have been better to increase that number to 8 as it is the risers cross section that prevented further reduction of the cell pot to pot distance as shown in Figure 9. Figure 10 presents the obtained busbar voltage drop of 85 Mv, a reduction of 49 mV over the 134 mV of the previous design despite the increase of the cell amperage.

This drastic reduction of the busbar voltage drop is obviously greatly contributing to the reduction of the cell power consumption. Another great advantage of reducing that component of the cell ohmic resistance is that it is not affecting the cell heat balance. Figures 11 to 13 demonstrate that the cell MHD is not negatively affected by the reduction of the pot to pot distance to 6.2 meters.

The design goal of the present study was to break the 11.0 kWh/kg barrier, as Table II indicated the new version of the 520 kA cell with 100% downstream side current extraction is predicted to consumed only 10.85 kWh/kg of Al produced, well below the 11.0 mark.

Comparison of the two cell design options

The comparison exercise presented in [1] is repeated here using the updated designs for both options. On the OPEX side, the discrepancy as increased to 0.15 kWh/kg now that the two cell designs are operated at the same “minimum” 2.8 cm of ACD. Clearly the busbar length requirement is what differentiate the most the two cell designs in favor of the 100% downstream side current extraction cell design option.

On the CAPEX side, a very crude comparison was made in [1] based on the length of potroom(s) required for a smelter to produce 1MM ton of Al per year. That number has not changed for the wider cell design option: at 95% current efficiency a 650 kA cell produces 4.974 ton Al per day so 550 cells are needed and with a 7.5 m of pot to pot distance, 4.2 km of potroom(s) are required to host them. On the other hand, that number has been improved for the 100% downstream current extraction cell design option. At 95% current efficiency, a 520 kA cell produces 3.980 ton Al per day so 688 cells are needed and with a 6.2 m of pot to pot distance, 4.3 km of potrooms are required to host them. Clearly increasing the cell amperage and at the same time reducing the pot to pot distance had a big impact on the CAPEX of that cell design option. Yet it is important to remember that the RCC busbar concept used in the wider cell design option doesn’t require a return line located 60 m away nor a set of independent rectifiers to power any external compensation busbar loops as it is the case for the 100% downstream side current extraction cell design using the ECC busbar concept.

Future work

It is the opinion of the author that further reduction of the cell energy consumption will probably have to come from the recovery of some of the heat loss by the cell. At the recent ICSOBA conference in Hamburg, such a heat recovery system (HRS) was presented by EGA [7]. Figure 14 from [7] presents the HRS concept, where heat can be extracted both from the cell exhaust gas and from the cell side walls. According to [7], 120 kW can on average be collected by the side wall heat exchangers. No data was provided for the conversion efficiency in [7], but in their TMS 2014 paper [8], Goodtech Recovery Technology that provided the HRS to EGA was talking of only 10%, admittedly on the conservative side. Based on [9], maybe assuming 20% of conversion efficiency is reasonable. On that basis, out of the 120 kW of cell heat loss collected, 24 kW can be converted back into electrical energy which for a 455 kA cell represents 53 mV or 0.165 kWh/kg.

On the cell exhaust gas heat recovery, it would be far more efficient to first increase the gas exhaust temperature. This could be achieved by reducing the area of the hood openings and also insulating the hoods and the fume plate in order to be able to decrease the gas exhaust rate and keep more of the anode panel heat loss in the exhaust gas. Also at the ICSOBA conference, the author presented a model that was developed to study the impact of such design changes [10] on the cell hooding system heat balance and the cell hooding HF capture efficiency. If the equivalent amount of heat collected on the cell side walls can be collected from the gas exhaust and converted into electrical energy, we are talking about a potential of 100 mV or about 0.31 kWh/kg of cell energy consumption reduction due to HRS having only 20% conversion efficiency

Discussion and Conclusions

Contrary to the author expectations one year ago, the present study has produced cell designs that have reached and in the second case broken the 11.0 kWh/kg cell energy consumption barrier. At 10.85 kWh/kg, at the time of writing this paper, the author ran out of design idea to further reduce that number without involving HRS. Even with HRS, the very low conversion rate of low grade heat energy into electrical energy means that HRS has the potential to further decrease the cell energy consumption by another 0.31 kWh/kg down to about 10.54 kWh/kg still 0.54 kWh/kg away from the next barrier to be broken, the 10.0 kWh/kg barrier.

Clearly, it would be far more efficient to use that captured low grade heat energy to preheat the alumina and/or the anodes or maybe use it to reduce the fuel consumption in the anode baking furnace. In such a case the 0.31 kWh/kg of cell energy consumption reduction becomes 1.55 kWh/kg, plenty to break the 10.0 kWh/kg barrier and even to start dreaming of breaking the next barrier!

References

[1] M. Dupuis, “Very low energy consumption cell designs: the cell heat balance challenge”, TMS Light Metals, 2018, to be published.

[2] M. Dupuis, “A new aluminium electrolysis cell busbar network concept”, Proceedings of 34th International ICSOBA Conference, Québec City, Canada, 3 – 6 October 2016, Paper AL39, Travaux No. 45, 883-890.

[3] M. Dupuis, “Low energy consumption cell design involving copper inserts and innovative busbar network layout”, TMS Light Metals, 2017, 693-703.

[4] M. Dupuis and B. Welch, “Designing cells for the future – wider and/or even higher amperage?”, ALUMINIUM, 93 (1/2), 2017, 45-49.

[5] M. Dupuis, “A new aluminium electrolysis cell busbar network concept”, Proceedings of 33rd International ICSOBA Conference, Dubai, UAE, 29 November – 1 December 2015, Paper AL21, Travaux No. 44, 699-708.

[6] M. Dupuis, “Presentation of a New Anode Stub Hole Design Reducing the Voltage Drop of the Connection by 50 mV”, VIII International Congress & Exhibition “Non-Ferrous Metals and Minerals”, Krasnoyarsk, Russia, 13 – 16 September 2016, https://drive.google.com/file/d/0Bwb-wQZ90LvBVF9WWWQ0LWZZdTQ/view .

[7] A. AlJasmi and A. AlZarouni, “Findings from operating a pot with heat recovery system”, Proceedings of 35th International ICSOBA Conference, Hamburg, Germany, 2 – 5 October 2017, Paper AL29, Travaux No. 46, 1071-1080.

[8] Y. M. Barzi, M. Assadi and H. M. Arvesen, “A novel heat recovery technology from an aluminum reduction cell side walls: experimental and theoretical investigations”, TMS Light Metals, 2014, 733-738.

[9] T. C. Hung, T. Y. Shai and S. K. Wang, “A review of organic rankine cycles (ORCs) for the recovery of low-grade waste heat”, Energy, 1997, Vol.22(7), 661-667.

[10] M. Dupuis, M. Pagé and F. Julien, “Development of an AUTODESK CFD-Based 3D Model of a Hall Héroult Cell Hooding System and HF Capture efficiency”, Proceedings of 35th International ICSOBA Conference, Hamburg, Germany, 2 – 5 October 2017, Paper AL07, Travaux No. 46, 835-850.

Author

Dr. Marc Dupuis is a consultant specialized in the applications of mathematical modeling for the aluminium industry since 1994, the year when he founded his own consulting company GeniSim Inc (www.genisim.com). Before that, he graduated with a Ph.D. in chemical engineering from Laval University in Quebec City in 1984, and then worked 10 years as a research engineer for Alcan International. His main research interests are the development of mathematical models of the Hall-Héroult cell dealing with the thermo-electric, thermo-mechanic, electro-magnetic and hydrodynamic aspects of the problem. He was also involved in the design of experimental high amperage cells and the retrofit of many existing cell technologies.

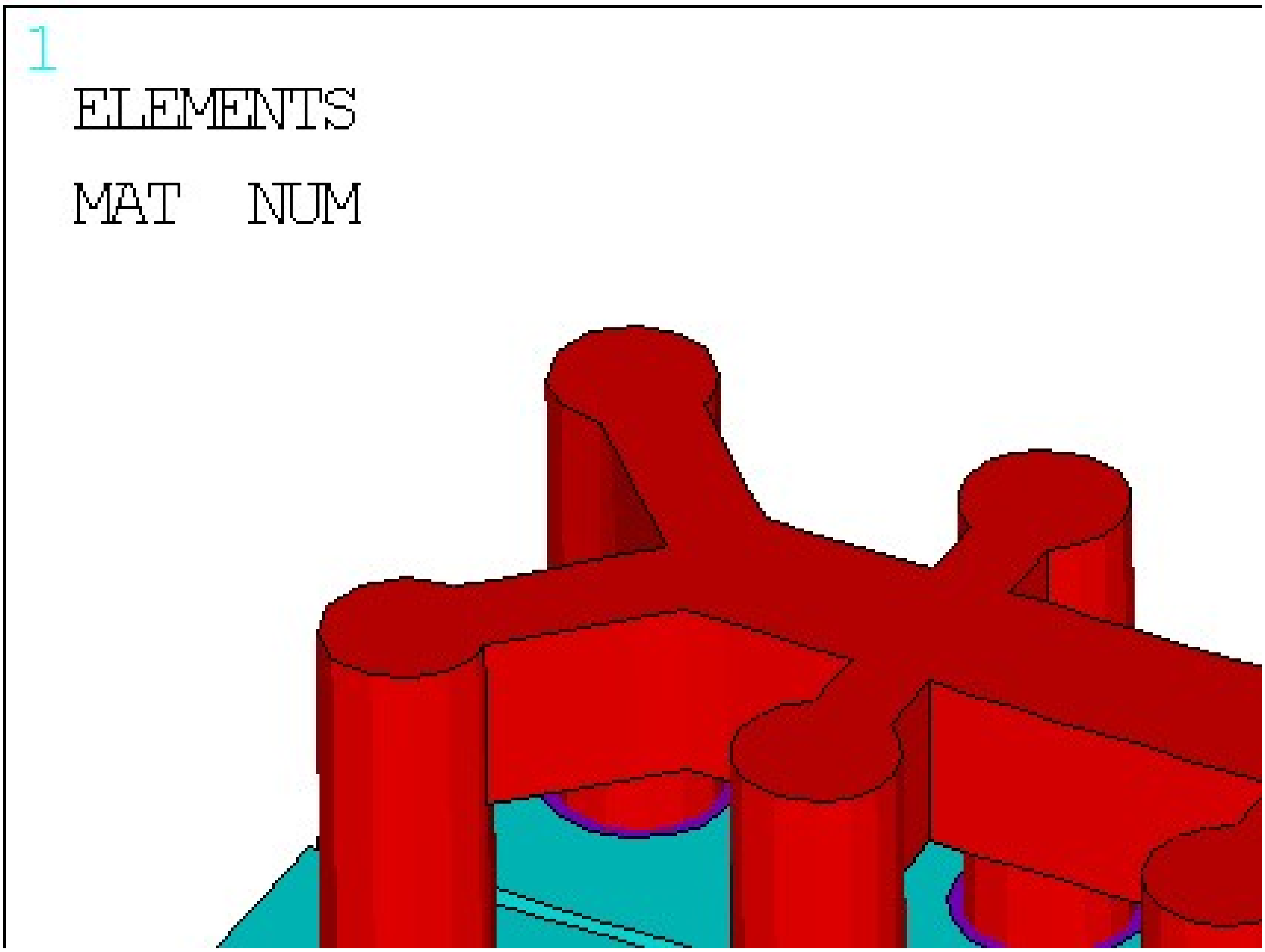

Figure 1: Topology of the 4 carbon blocks per anode, 3 stubs per carbon block new anode design

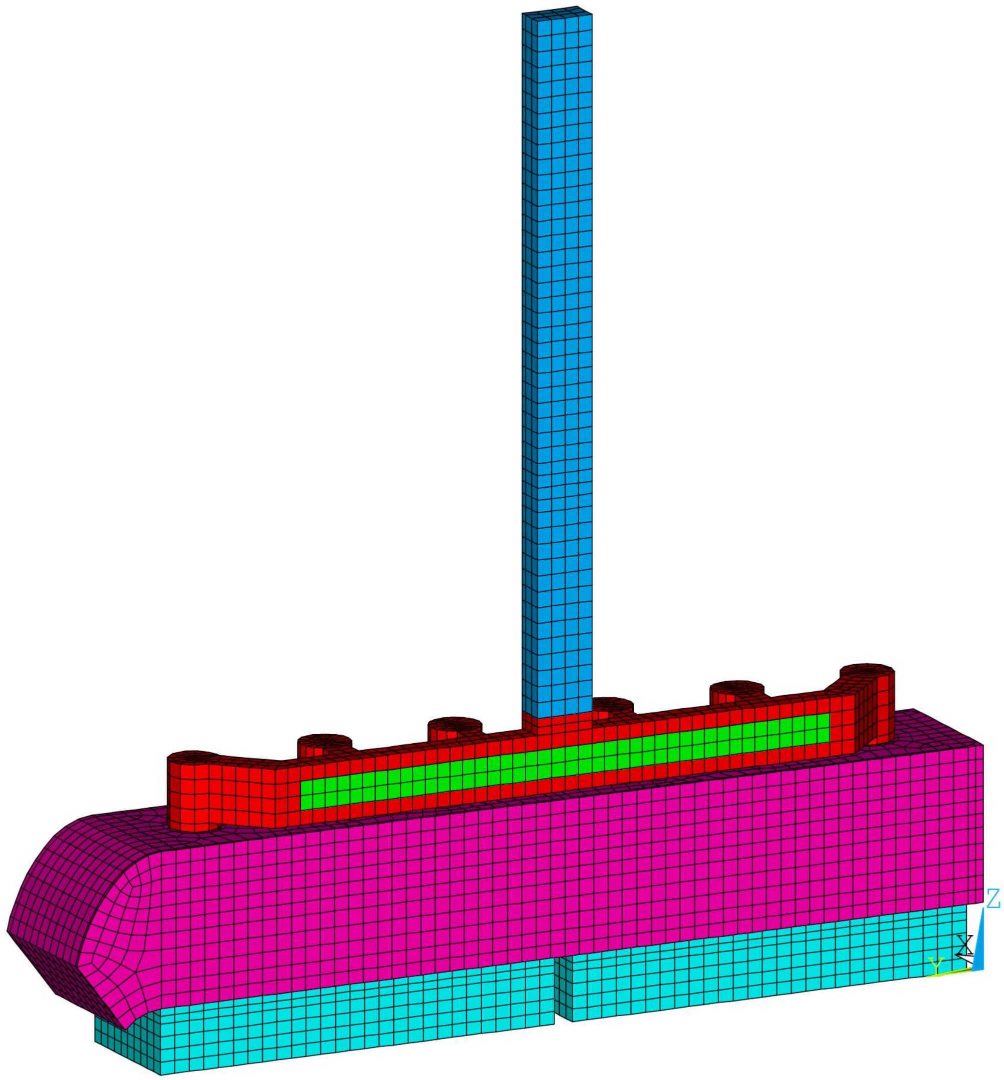

Figure 2: Half anode model mesh showing the copper insert in green

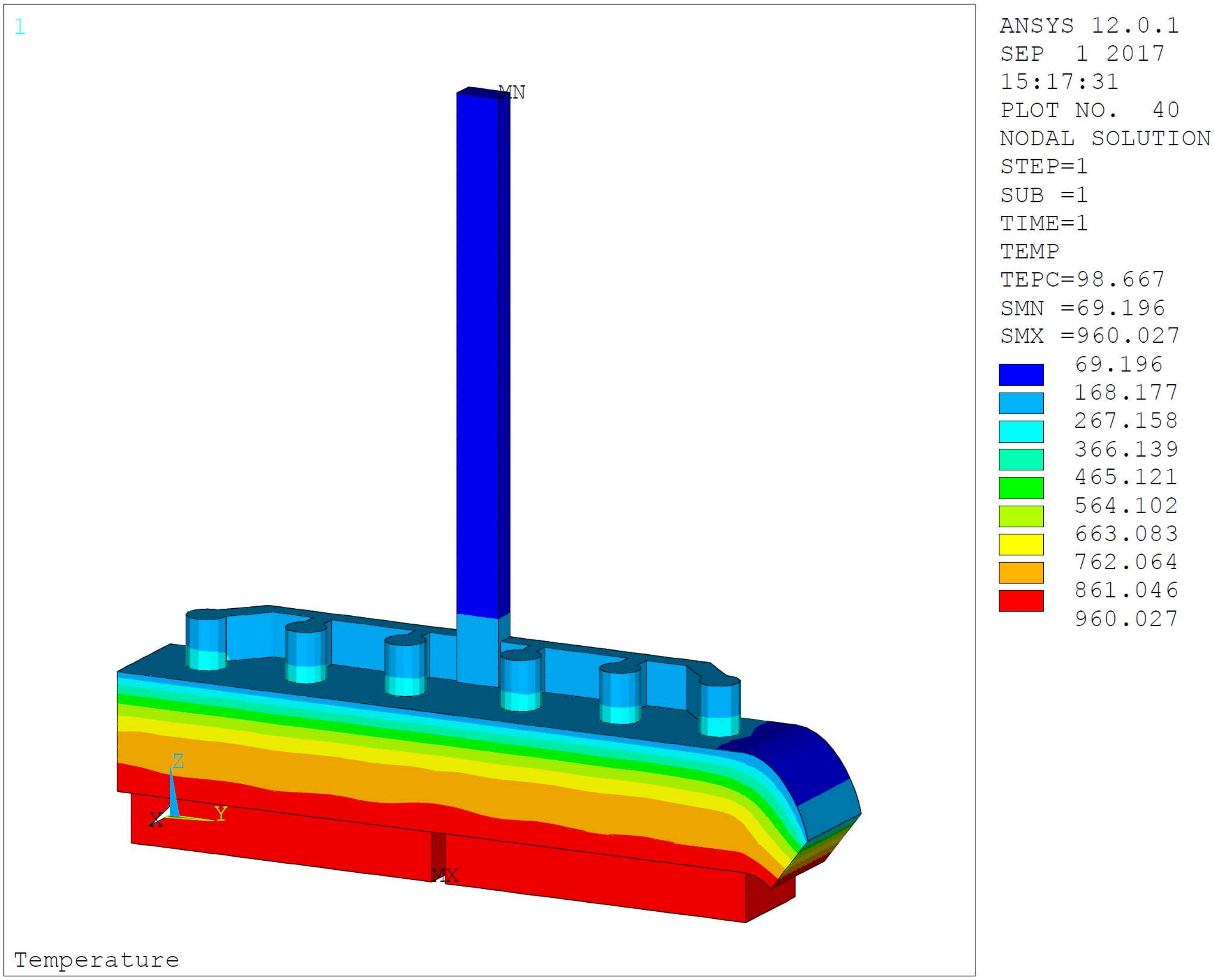

Figure 3: Anode model temperature solution

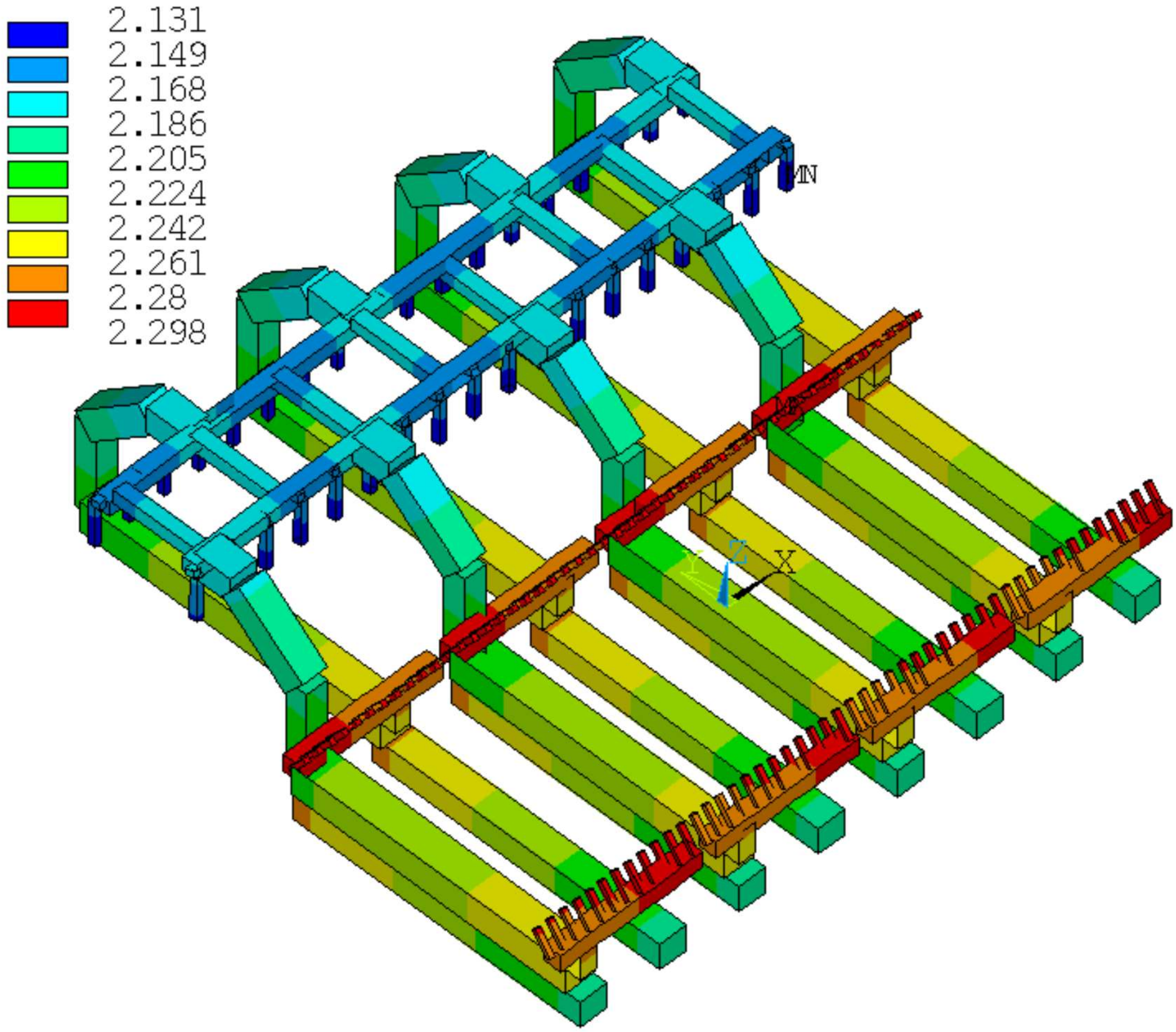

Figure 4: Wider 650 kA model predicted busbar voltage drop

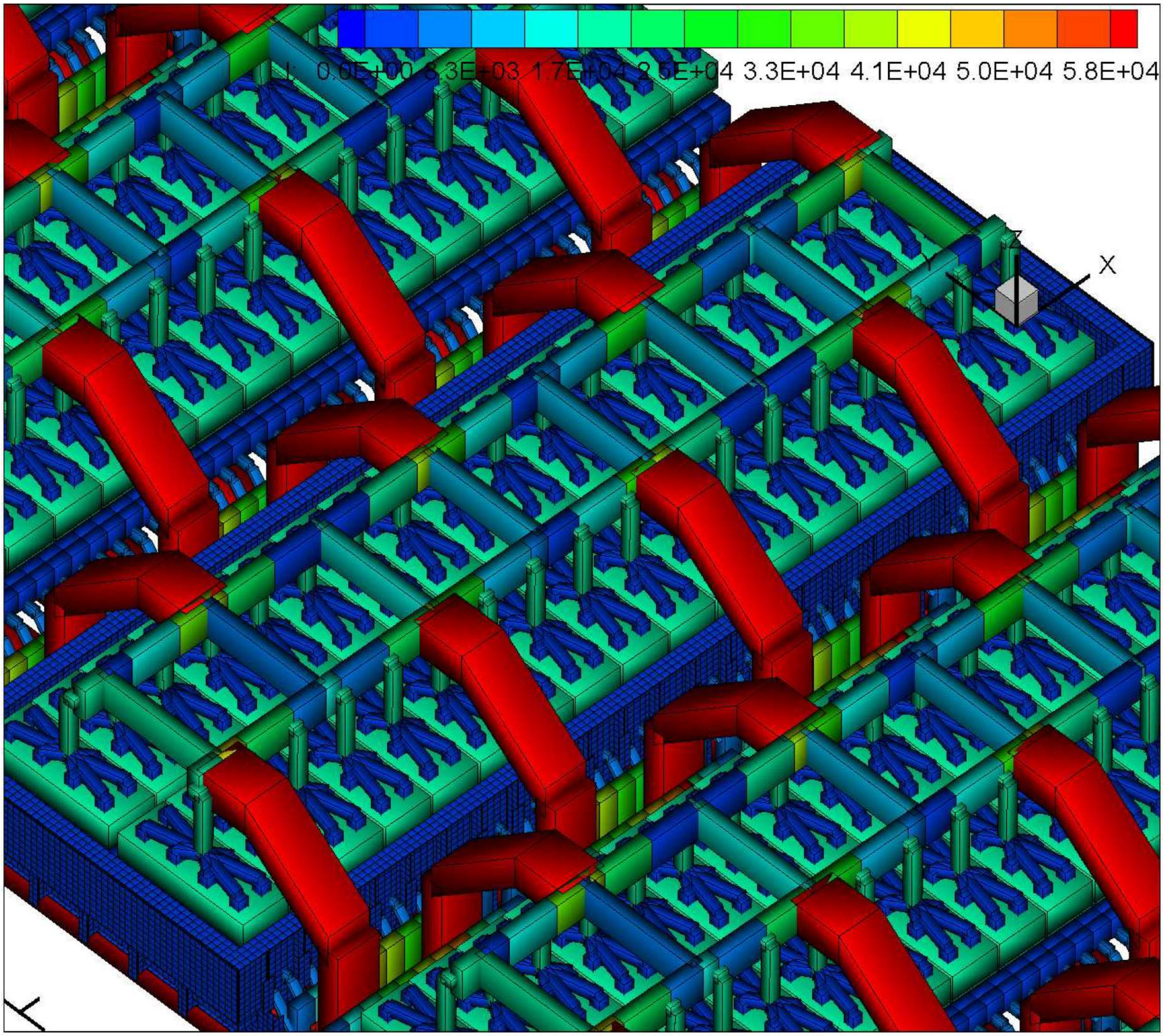

Figure 5: Wider 650 kA 8 risers RCC busbar network MHD-Valdis model setup

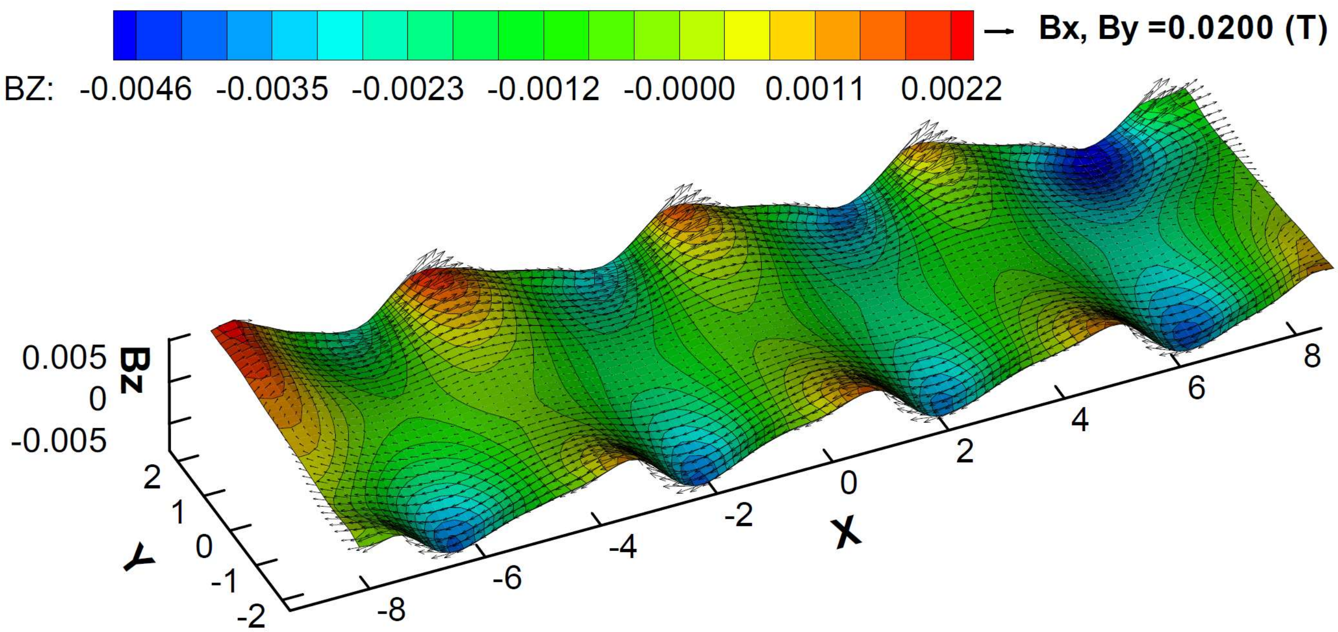

Figure 6: Wider 650 kA 8 risers RCC busbar network MHD-Valdis model BZ prediction

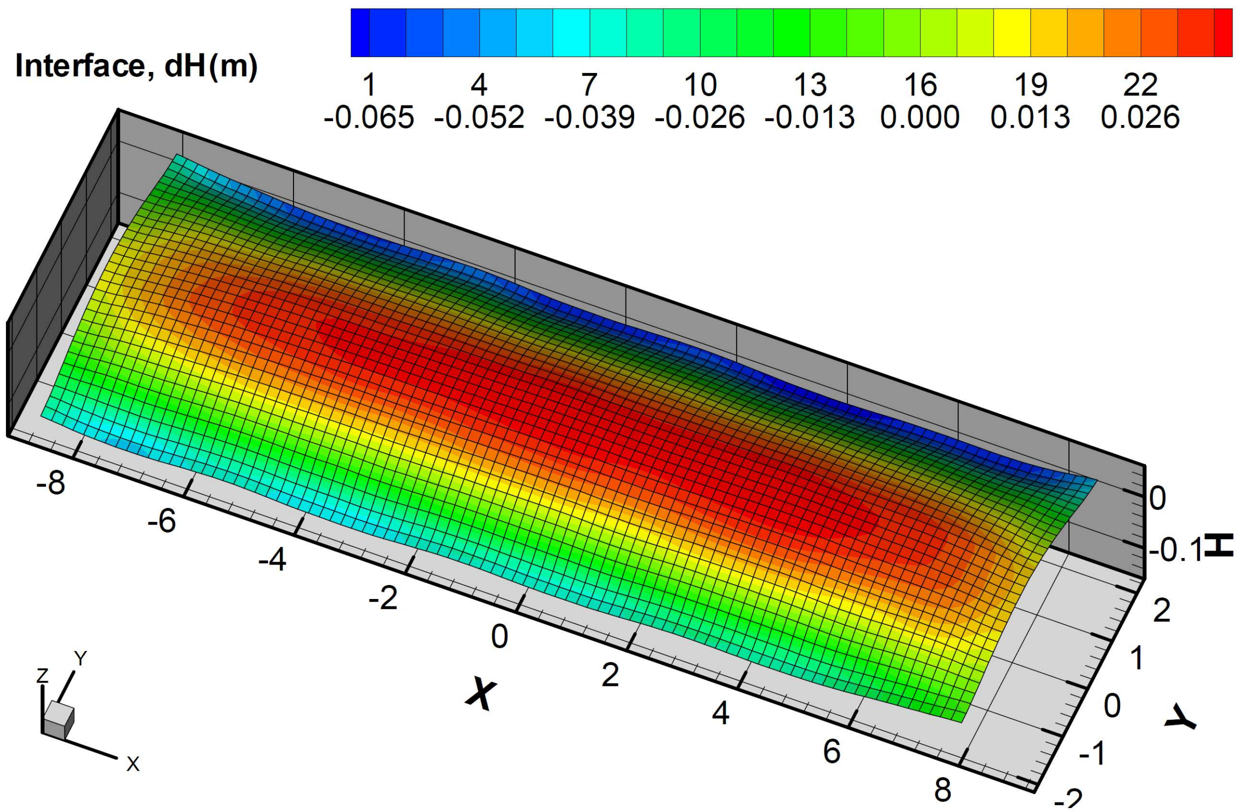

Figure 7: Wider 650 kA 8 risers RCC busbar network MHD-Valdis model bath-metal interface prediction

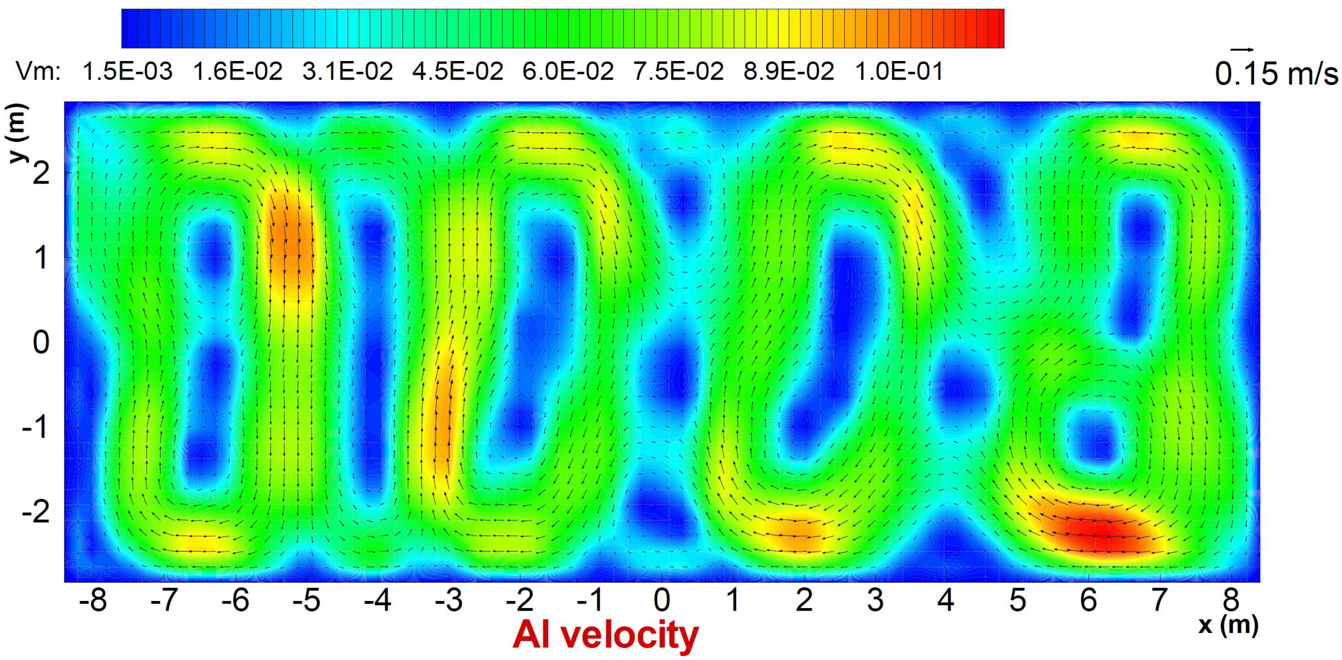

Figure 8: Wider 650 kA 8 risers RCC busbar network MHD-Valdis model metal flow field prediction

Table I: Design 1, Wider 650 kA cell using RCC busbar design

Amperage	762.5 kA	650 kA	650 kA
Nb. of anodes	48	48	36
Anode size	2.6m X .65m	2.6m X .65m	2.6m X .86m
Nb. of anode studs	4 per anode	4 per anode	12 per anode
Anode stud diameter	21.0 cm	24.0 cm	16.0 cm
Anode cover thickness	15 cm	24 cm	25 cm
Nb. of cathode blocks	24	24	24
Cathode block length	5.37 m	5.37 m	5.37 m
Type of cathode block	HC10	HC10	HC10
Collector bar size	20 cm X 12 cm	20 cm X 15 cm	20 cm X 15 cm
Type of side block	HC3	HC3	HC3
Side block thickness	7 cm	7 cm	7 cm
ASD	25 cm	25 cm	25 cm
Calcium silicate thickness	3.5 cm	6.0 cm	6.0 cm
Inside potshell size	17.02 X 5.88 m	17.02 X 5.88 m	17.02 X 5.88 m
ACD	3.0 cm	2.8 cm	2.8 cm
Excess AlF_3	11.50%	11.50%	11.50%
Anode drop (A)	347 mV	296 mV	252 mV
Cathode drop (A)	118 mV	109 mV	109 mV
Busbar drop (A)	300 mV	220 mV	170 mV
Anode panel heat loss (A)	553 kW	327 kW	339 kW
Cathode total heat loss (A)	715 kW	499 kW	482 kW
Operating temperature (D/M)	968.9 °C	967.0 °C	966.5 °C
Liquidus superheat (D/M)	10.0 °C	8.1 °C	7.6 °C
Bath ledge thickness (A)	6.82 cm	11.86 cm	14.25 cm
Metal ledge thickness (A)	1.85 cm	3.38 cm	4.58 cm
Current efficiency (D/M)	95.14%	94.80%	94.90%
Internal heat (D/M)	1328 kW	832 kW	804 kW
Energy consumption	12.85 kWh/kg	11.3 kWh/kg	11.0 kWh/kg

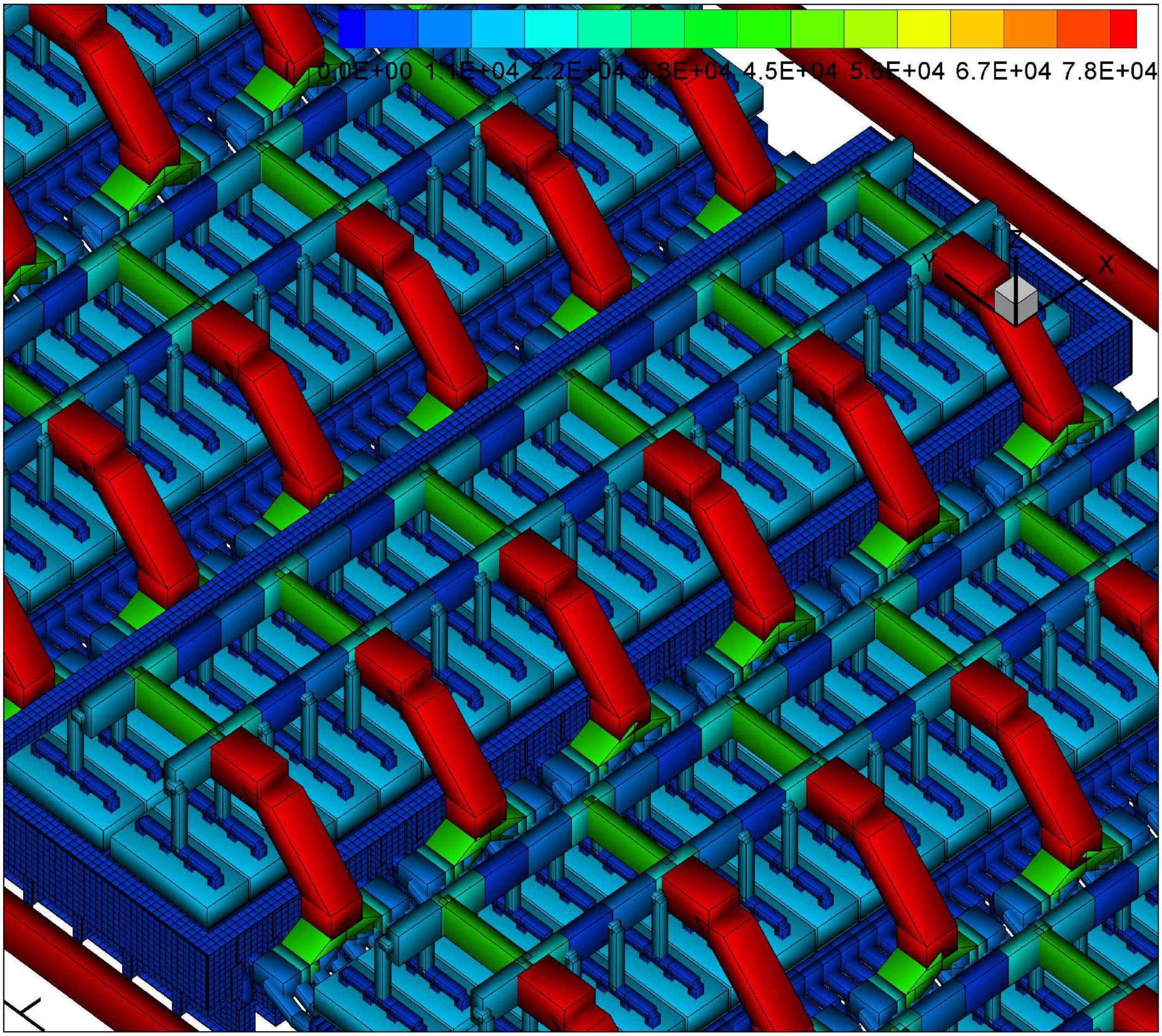

Figure 9: 520 kA 6 risers 100% downstream current extraction cell with ECC busbar network, MHD-Valdis model setup

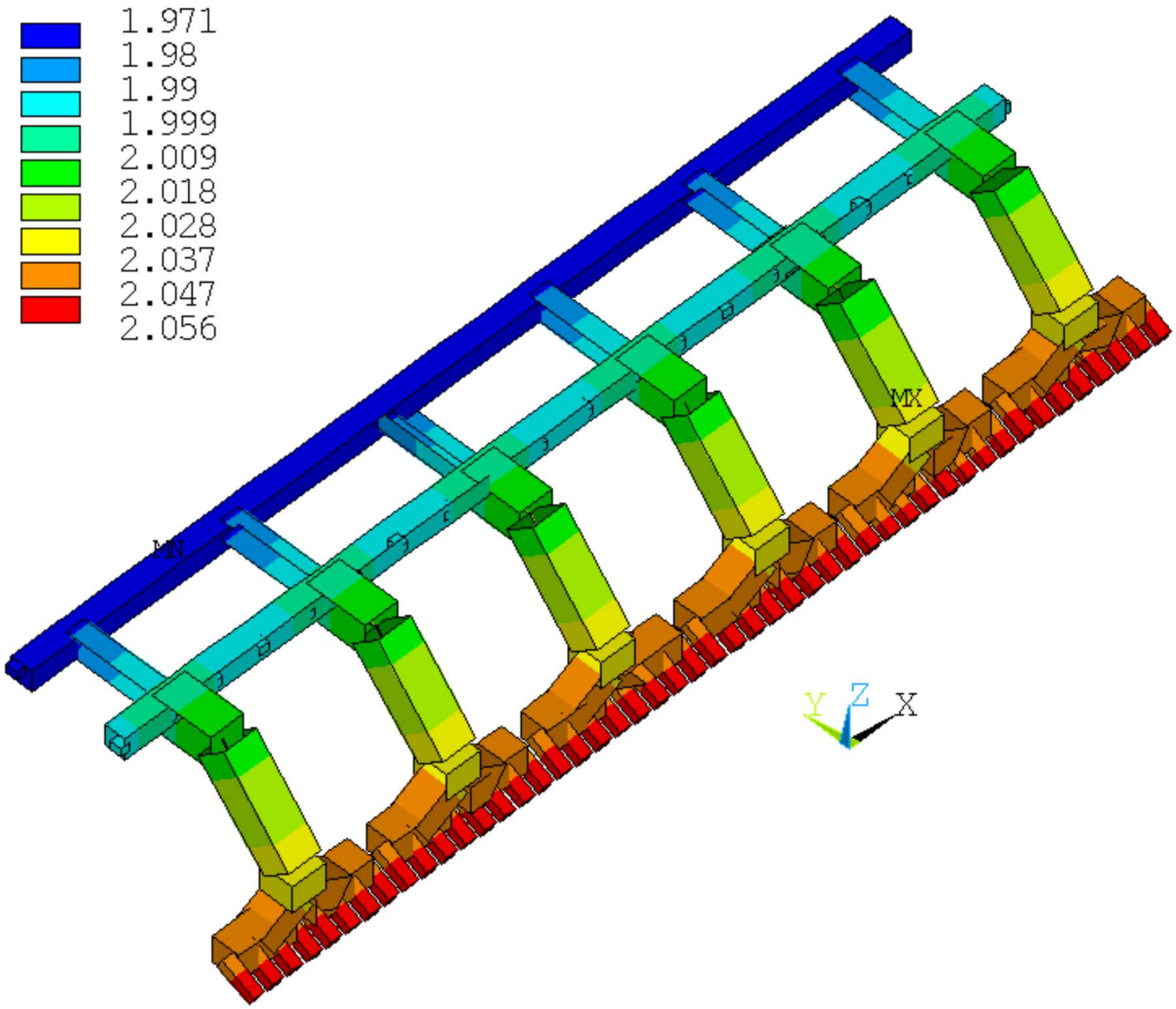

Figure 10: 520 kA 6 risers 100% downstream current extraction cell with ECC busbar network predicted voltage drop

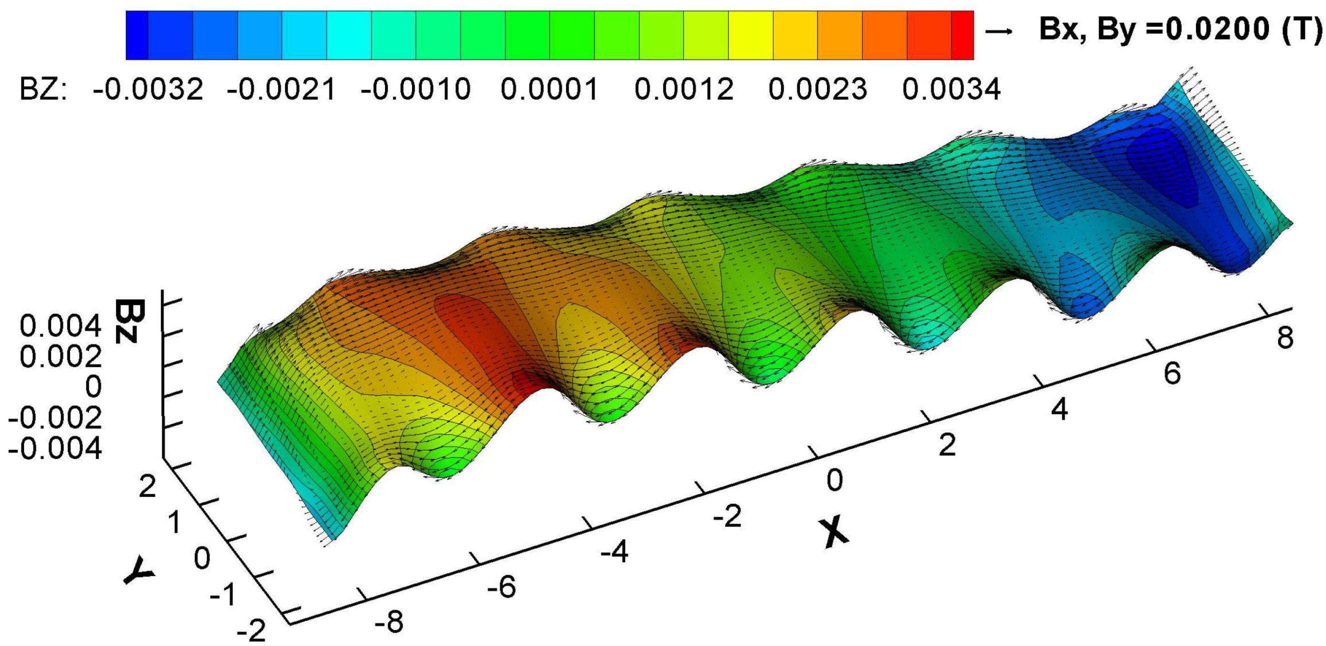

Figure 11: 520 kA 6 risers 100% downstream current extraction cell with ECC busbar network predicted BZ

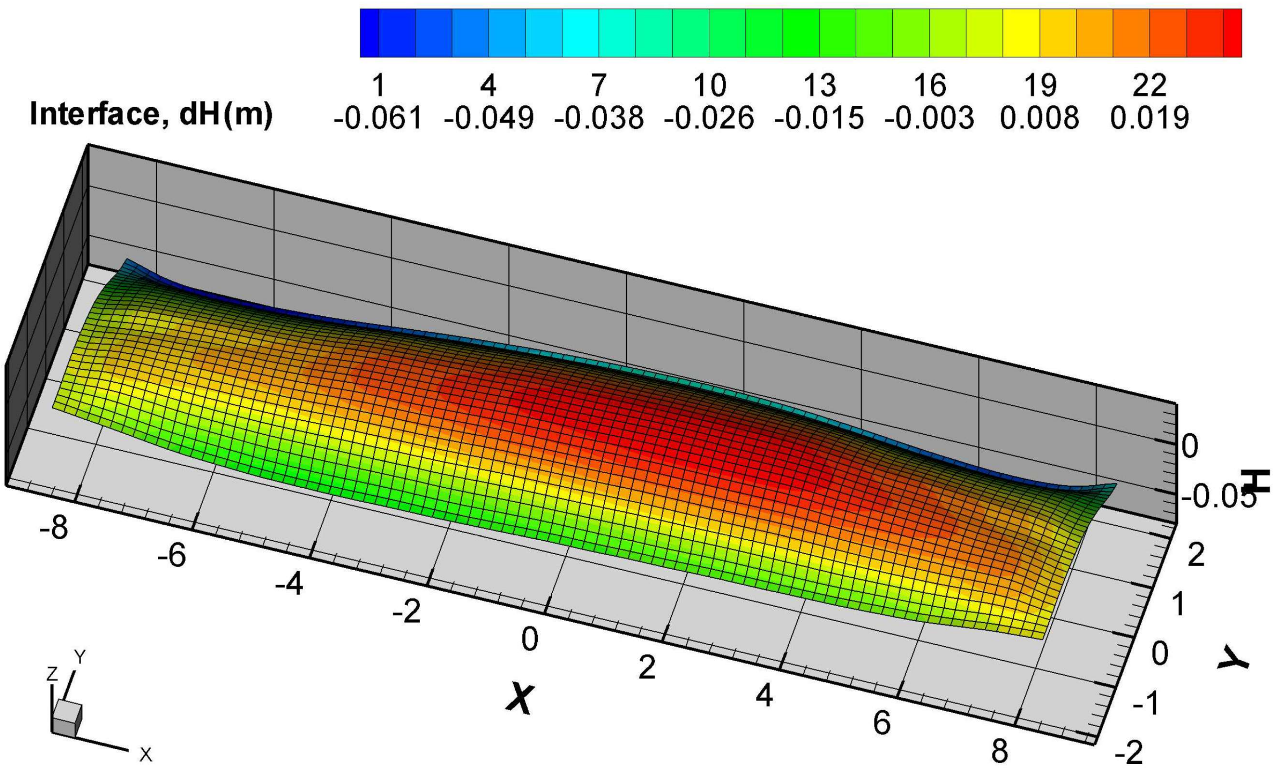

Figure 12: 520 kA 6 risers 100% downstream current extraction cell with ECC busbar network predicted bath-metal interface

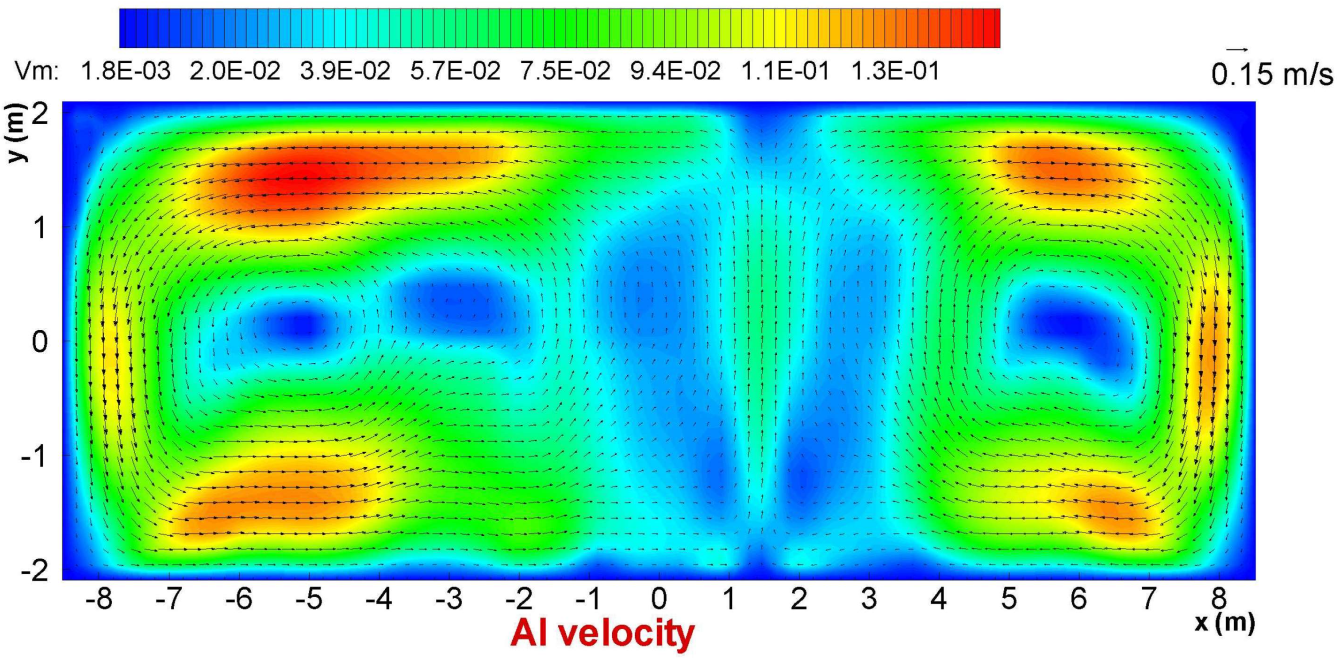

Figure 13: 520 kA 6 risers 100% downstream current extraction cell with ECC busbar network predicted metal flow field

Table II: Design 2, 520 kA cell with 100% downstream side current extraction

Amperage	600 kA	500 kA	520 kA
Nb. of anodes	48	64	64
Anode size	2.0m X .665m	1.95m X .5m	1.95m X .5m
Nb. of anode studs	4 per anode	4 per anode	4 per anode
Anode stud diameter	17.5 cm	17.5 cm	17.5 cm
Anode cover thickness	10 cm	20 cm	20 cm
Nb. of cathode blocks	24	24	24
Cathode block length	4.17 m	4.17 m	4.17 m
Type of cathode block	HC10	HC10	HC10
Collector bar size	20 cm X 10 cm	20 cm X 20 cm	20 cm X 20 cm
Type of side block	SiC	HC3	HC3
Side block thickness	7 cm +	7 cm	7 cm
ASD	28 cm	30 cm	30 cm
Calcium silicate thickness	3.5 cm	6.0 cm	6.0 cm
Inside potshell size	17.8 X 4.85 m	17.8 X 4.85 m	17.8 X 4.85 m
ACD	3.5 cm	3.2 cm	2.8 cm
Excess AlF_3	12.00%	12.00%	12.00%
Anode drop (A)	318 mV	238 mV	248 mV
Cathode drop (A)	104 mV	123 mV	128 mV
Busbar drop (A)	311 mV	134 mV	85 mV
Anode panel heat loss (A)	449 kW	292 kW	295 kW
Cathode total heat loss (A)	692 kW	402 kW	404 kW
(D/M)	964.8 °C	958.4 °C	958.3 °C
Liquidus superheat (D/M)	11.8 °C	5.4 °C	5.3°C
Bath ledge thickness (A)	6.36 cm	11.84 cm	11.83 cm
Metal ledge thickness (A)	1.76 cm	3.48 cm	3.46 cm
Current efficiency (D/M)	96.4%	96.3%	96.5%
Internal heat (D/M)	1140 kW	699 kW	701 kW
Energy consumption	13.26 kWh/kg	11.2 kWh/kg	10.85 kWh/kg

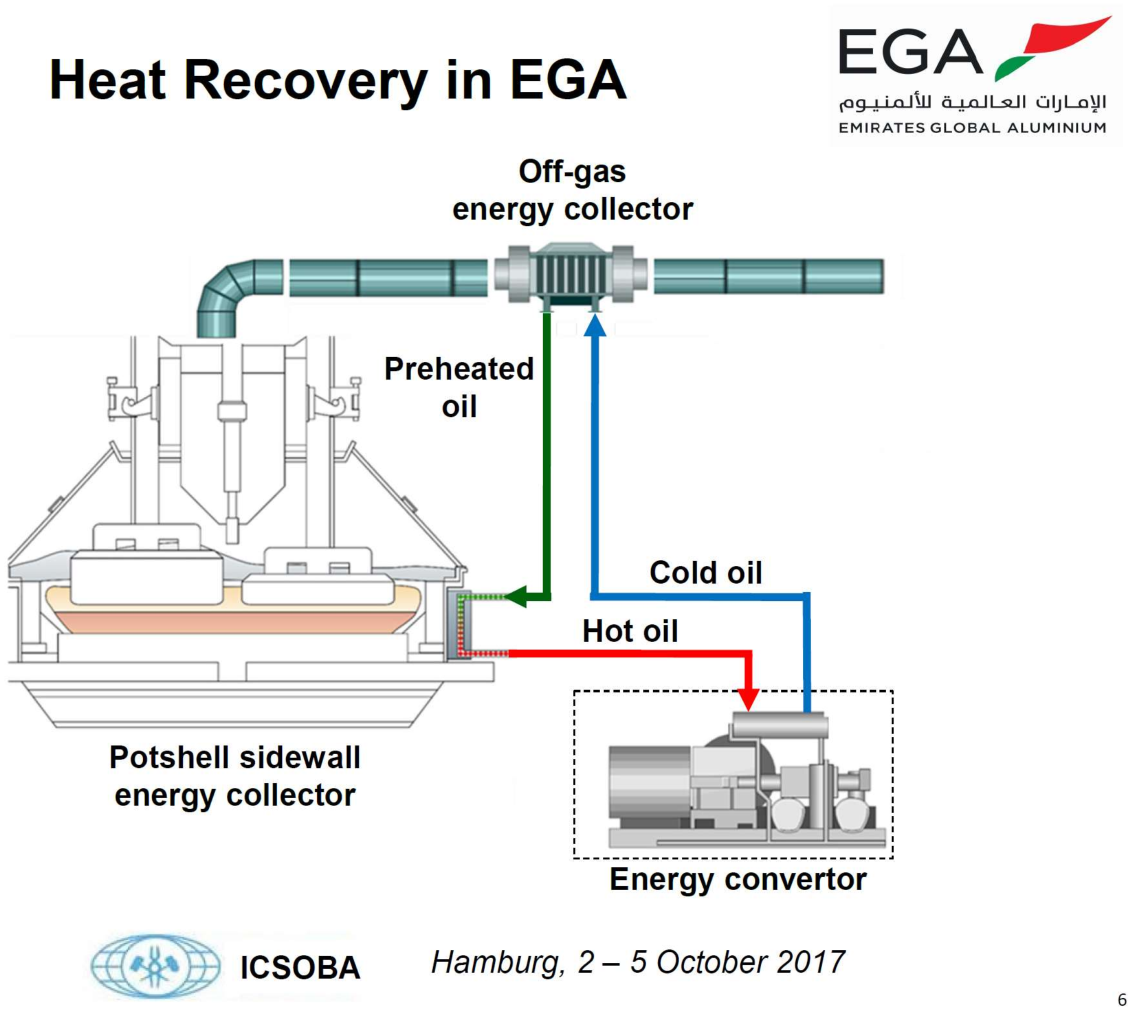

Figure 14: Heat recovery system (HRS) tested by EGA, extracted from [7] presentation